

CHARACTERISTIC PROPERTIES OF THE THREE-HALF-TURN-ANTENNA-DRIVEN RF DISCHARGE IN THE URAGAN-3M TORSATRON

V.V. Chechkin, L.I. Grigor'eva, D.L. Grekov, R.O. Pavlichenko, A.V. Lozin, A.A. Kasilov, A.A. Beletskii, M.M. Kozulya, A.Ye. Kulaga, N.V. Zamanov, I.K. Tarasov, Yu.K. Mironov, V.S. Romanov, V.S. Voitsenya

Institute of Plasma Physics NSC KIPT, Kharkov, Ukraine

In the $\lambda = 3$ Uragan-3M torsatron hydrogen plasma is heated by RF fields in the Ålfven range of frequencies ($\omega \lesssim \omega_{ci}$). Plasma with the mean density \bar{n}_e units of 10^{12} cm^{-3} is produced by the frame antenna and used as an initial plasma ("target") to produce and heat a denser plasma (up to $\bar{n}_e \sim 10^{13} \text{ cm}^{-3}$) by means of the shorter wavelength three-half-turn antenna with azimuthal currents. Characteristics of the three-half-turn-antenna-driven discharge are studied experimentally depending on the RF power fed to the antenna and initial plasma parameters.

PACS: 52.25.Fi, 52.55.Hc, 52.55.Pi, 52.70.Pi

INTRODUCTION

In the Uragan-3M torsatron (U-3M; $\lambda = 3 / m = 9$, $R_0 = 100 \text{ cm}$, $\bar{a} \approx 12 \text{ cm}$, $\iota(a)/2\pi \approx 0,3$) hydrogen plasma is produced and heated by RF fields in the Ålfven range of frequencies ($\omega \lesssim \omega_{ci}$). The toroidal magnetic field $B_\phi \lesssim 1 \text{ T}$ is produced by the helical coils only, and the entire magnetic system is enclosed into a large 5 m diameter vacuum chamber, so that an open helical divertor is realized. The initial plasma with the line-averaged electron density (mean density) \bar{n}_e of units 10^{12} cm^{-3} is produced by an unshielded frame-like antenna (FA) with a broad spectrum of parallel wavelengths λ_{\parallel} and large parallel currents [1]. In the regime where $\bar{n}_e \sim (1\dots3) \times 10^{12} \text{ cm}^{-3}$, $T_e \gtrsim 100 \text{ eV}$ the plasma is weakly collisional and its investigation is of spetial interest for modeling physical processes in large fusion devices [2, 3].

The FA-produced plasma is also used as a target to produce and heat a denser plasma ($\bar{n}_e \sim 10^{13} \text{ cm}^{-3}$) with the help of another, shorter wavelength antenna with azimuthal currents (three-half-turn antenna, THTA) [4, 5].

In this work being a continuation of [6] characteristics of the THTA-driven discharge are studied depending on the RF power fed to the antenna and initial (target) plasma parameters.

1. EXPERIMENTAL CONDITIONS

THTA (Fig. 1) partly covers the plasma column toroidally over 30 cm. In comparison with FA, the parallel conductors of THTA are removed farther away from the plasma to reduce undesirable excitation of the slow Ålfven wave at the periphery, while the transversal conductors embrace a larger part of the plasma column for a more efficient excitation of the fast wave [7, 8].

The excitation maximum in the parallel wavelength spectrum generated by the antenna falls at $\lambda_{\parallel} \approx 30 \text{ cm}$.

The antenna is fed by the Kaskad-2 (K2) RF oscillator with the frequency $\omega_2/2\pi = 8.7 \text{ MHz}$

($\omega_2 = 0.8\omega_{ci}(0)$) and maximum RF power fed to the antenna $P_{K2} \approx 350 \text{ kW}$ at the anode voltage $U_{K2} = 9 \text{ kV}$. The resonance local plasma density corresponding to the excitation maximum at $\lambda_{\parallel} \approx 30 \text{ cm}$ is $\sim 10^{13} \text{ cm}^{-3}$.

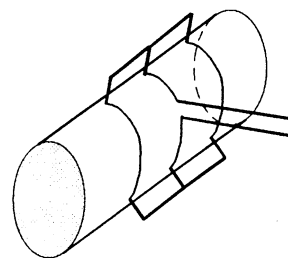


Fig. 1. Schematic representation of the three-half-turn antenna [5]

The density \bar{n}_e was measured by a 2 mm interferometer. The electron temperature (radiation temperature, T_e^{rad}) was estimated by the intensity of the 2nd harmonic ECE from the central region. Taking into account a probable radial density profile, the maximum \bar{n}_e for which the temperature could be estimated by ECE cannot exceed $\sim (6\dots7) \times 10^{12} \text{ cm}^{-3}$ because of the cut-off effect. Qualitatively, an idea on the level of plasma loss can be derived from the value of the plasma divertor flow (PDF) that is presented by the ion saturation current I_s to a Langmuir probe crossed by the flow in a gap between the helical coils [2].

The fueling gas (hydrogen) was admitted continuously into the vacuum chamber at the initial pressure of $p \sim 10^{-5} \text{ Torr}$.

The initial FA-driven RF discharge can stay in two regimes depending on the pressure p and the RF power P_{K1} fed to the antenna [6]. The regime 1 is characterized by a low density, $\bar{n}_e \sim (1\dots3) \times 10^{12} \text{ cm}^{-3}$, a high T_e^{rad} (up to $\sim 700 \text{ eV}$ [6]) and a large plasma loss. In the regime 2 a higher density is attained (up to $\bar{n}_e \sim 7 \times 10^{12} \text{ cm}^{-3}$) with a lower level of ECE and a lower plasma loss. With a low RF power P_{K1}

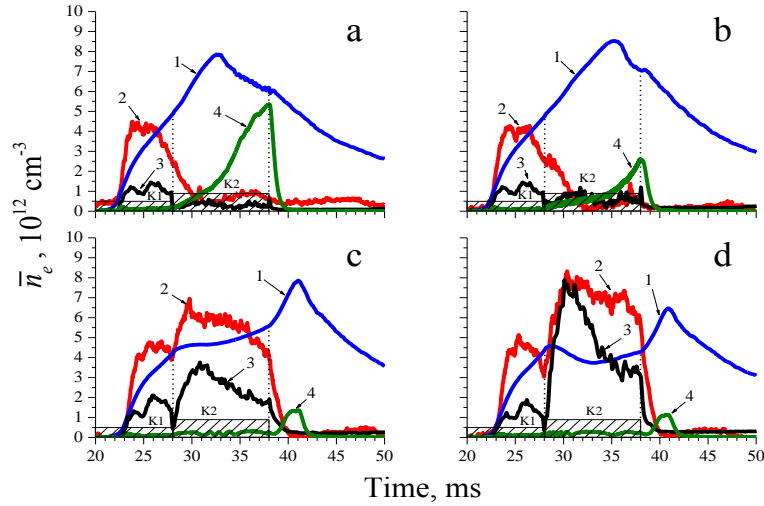


Fig. 2. Time evolution of 1 – \bar{n}_e ; 2 – ECE; 3 – PDF (current I_s) and 4 – line CIII intensity at fixed $U_{K1} = 5 \text{ kV}$ and (a) $U_{K2} = 5.0 \text{ kV}$, (b) 6.0 kV , (c) 7.5 kV , (d) 8.5 kV . The mean electron density is in units of 10^{12} cm^{-3} , while the other signals are in arbitrary units

(the oscillator anode voltage is $U_{K1} \sim 5 \dots 7 \text{ kV}$) during the RF pulse, as the density increases, the discharge goes from the regime 1 to the regime 2. With a higher power the regime 1 spreads over the whole RF pulse.

2. DISCHARGE EVOLUTION DEPENDING ON THE RF POWER FED TO THTA

With a fixed $U_{K1} = 5 \text{ kV}$ ($P_{K1} \approx 45 \text{ kW}$) U_{K2} was raised from 5 kV ($\approx 150 \text{ kW}$) to 8.5 kV ($\approx 300 \text{ kW}$). The moment $t_0 = 28 \text{ ms}$ of K1 switched off, with the initial discharge going from the regime 1 to the regime 2, coincided with the moment t_1 of K2 switched on. With $p = 1.05 \times 10^{-5} \text{ Torr}$, the shot-to-shot variation of the initial density \bar{n}_{e0} was within $\sim (4 \dots 5) \times 10^{12} \text{ cm}^{-3}$.

With the lowest value $U_{K2} = 5.0 \text{ kV}$, $\bar{n}_e(t)$ continues to increase and traverses $\max \bar{n}_e \sim 8 \times 10^{12} \text{ cm}^{-3}$ at the moment 32.5 ms (Fig. 2,a). ECE goes on falling to the level comparable with the interference. The cooling of electrons is confirmed by a loss decrease (by PDF) and a rise of the impurity carbon line CIII emission. With stepping up U_{K2} (6 kV , see Fig. 2,b), the start of plasma heating (ECE rise at the beginning of the K2 pulse) results in a loss increase (a PDP rise) with corresponding slowing down of the density rise and $\max \bar{n}_e$ shift toward RF pulse termination (35 ms in Fig. 2,b). Beginning in $U_{K2} \sim 7 \text{ kV}$ (see Fig. 2,c, 7.5 kV), ECE and PDF already appreciably exceed their initial values, and the density rise is slowed down so that $\max \bar{n}_e \sim 8 \times 10^{12} \text{ cm}^{-3}$ is no more reached within the THTA pulse, and the density can rise only to $\bar{n}_e \approx 5.6 \times 10^{12} \text{ cm}^{-3}$. With $U_{K2} \gtrsim 8 \text{ kV}$ (see Fig. 2,d, 8.5 kV), juxtaposing time behaviors of ECE, PDP and \bar{n}_e , one can conclude that with the increase of the heating power and energetic electrons content, the plasma loss becomes so high that it cannot be balanced by ionization of neutrals inflowing from the ambient

volume at the adjusted pressure p . This results in a density decrease in the 1st half of the THTA pulse to $\bar{n}_e \approx 3.7 \times 10^{12} \text{ cm}^{-3}$, thus resembling plasma behavior in the regime 1 of the FA-driven discharge [6]. A considerable electron heating in Figs. 2,c,d conditions is evidenced by not only high levels of ECE and PDF but by a low level of the CIII emission in the active phase of the discharge and occurrence of the “recombination” maximum of this emission after K2 switched off.

Note that under Fig. 2,d conditions, PDF, after passing over the maximum in the 1st half of the THTA pulse, drops more quickly than ECE, while \bar{n}_e , after passing over a minimum in the 1st half of the RF pulse, increases to $\approx 4.3 \times 10^{12} \text{ cm}^{-3}$ (see, also, Fig. 5,a in Sec. 4). This means that the plasma loss decreases over the THTA pulse and the discharge regime changes toward a better plasma confinement with a relatively high electron temperature.

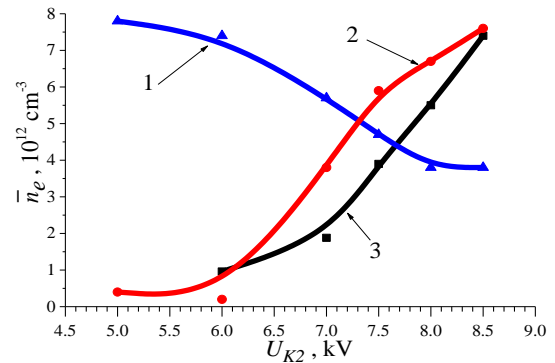


Fig. 3. 1 – mean electron density \bar{n}_e ; 2 – ECE; 3 – PDF (I_s) versus anode voltage U_{K2} at fixed $U_{K1} = 5 \text{ kV}$. The values of \bar{n}_e , ECE and I_s were taken at $t = 32.5 \text{ ms}$ where \bar{n}_e took a maximum at $U_{K2} = 5 \text{ kV}$ (see Fig. 2,a). The mean electron density is in units of 10^{12} cm^{-3} , while the other quantities are in arbitrary units

A short-time \bar{n}_e increase after RF pulse termination with a subsequent slower density decay that is observed in Fig. 2,c ($U_{K2} = 7.5$ kV) and at higher U_{K2} (see Fig. 2,d; 8.5 kV) result from a plasma loss decrease after the end of RF heating. This is evidenced by a rapid (~ 1 ms) PDF drop. With this, the temperature of the cooling electrons still is high enough to ionize neutrals that enter continuously the confinement volume (see, e.g., [9]). The absence of the “recombination” maximum of the CIII emission as well as the absence of the afterglow plasma density increase after K2 switched

off in high density regimes (Figs. 2,a,b) evidence the presence of a low electron temperature before RF off.

In Fig. 3 plots are shown of ECE, PDF (current I_s) and \bar{n}_e against U_{K2} made from the data similar to those shown in Fig. 2. The values of the parameters were taken at the moment 32.5 ms, where \bar{n}_e passed over the maximum at the lowest anode voltage $U_{K2} = 5$ kV (see Fig. 2,a). It is seen that with P_{K2} (voltage U_{K2}) increasing, ECE, plasma loss and \bar{n}_e behave qualitatively like behavior of these parameters in the FA-driven discharge when going from the regime 2 to the regime 1 (Fig. 5 in [6]).

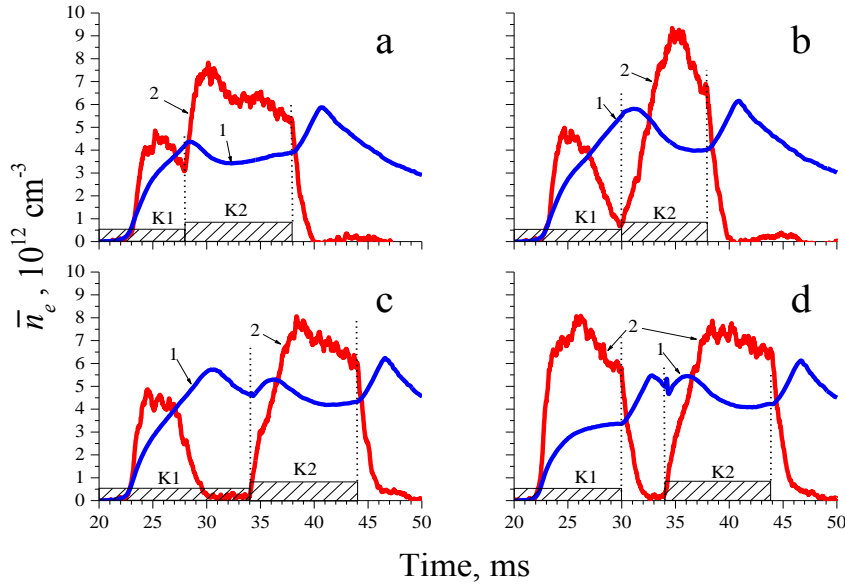


Fig. 4. Time evolution of 1 – mean electron density \bar{n}_e and 2 – 2nd harmonic ECE from the central region at fixed $U_{K1} = 5.0$ kV, $U_{K2} = 9.0$ and with (a) $t_0 = t_1 = 28$ ms; (b) $t_0 = t_1 = 30$ ms; (c) $t_0 = t_1 = 34$ ms; (d) $t_0 = 30$ ms, $t_1 = 34$ ms. The mean electron density is in units of 10^{12} cm^{-3} , while the other signals are in arbitrary units

3. INITIAL ELECTRON TEMPERATURE EFFECT ON PLASMA HEATING WITH THTA

With fixed $U_{K1} = 5$ kV ($P_{K1} \approx 45$ kW), $U_{K2} = 9$ kV (≈ 350 kW) and $p = 1.05 \times 10^{-5}$ Torr, the time t_0 was increased from shot to shot. Accordingly, the moment $t_1 = t_0$ was shifted (Figs. 4,a-c), and the FA-driven RF discharge went from the regime 1 with a high initial ECE (see Fig. 4,a: $t_0 = 28$ ms, ECE ≈ 3.2 a.u.) to the regime 2 with initial ECE decreasing to ≈ 0.7 a.u. at $t_0 = 30$ ms (see Fig. 4,b) and to the level ≈ 0.2 a.u. comparable with interference at $t_0 = 34$ ms (see Fig. 4,c). Both the initial density \bar{n}_{e0} and the density \bar{n}_e corresponding to the measured ECE maximum with THTA in operation changed within relatively small limits $\approx (4.2 \dots 5.5) \times 10^{12} \text{ cm}^{-3}$ and were lower than the values $\bar{n}_e \sim (7 \dots 8) \times 10^{12} \text{ cm}^{-3}$, where the cut off effect on the ECE level supposedly expected.

As is seen in Figs. 4,a-c, the maximum ECE attained with THTA in operation, weakly depends on the initial value, amounting $\approx 8-9$ a.u. with a discharge regime similar to the regime 1 of the FA-driven discharge.

It is appropriately also to present here the data taken from other measurement session where $U_{K1} = 6$ kV, $U_{K2} = 9$ kV (see Fig. 4,d). Here the moments $t_0 = 30$ ms and $t_1 = 35$ ms were separated, so that the oscillator K2 was switched on in the phase of the afterglow plasma produced by FA with an ultimately low initial ECE. In these conditions the maximum ECE attained with THTA in operation (7.5 a.u.) also is close to the values attained in the $t_0 = t_1$ conditions.

4. INITIAL PLASMA DENSITY EFFECT ON DENSITY AND HEATING OF THE THTA-DRIVEN PLASMA

As in Sec. 3 with respect to the initial ECE, with fixed $U_{K1} = 5$ kV and $U_{K2} = 9$ kV various \bar{n}_{e0} values were selected by changing t_0 and t_1 . In contrast to Sec. 2 and 3, here the measurements were carried out at the higher $p = 1.15 \times 10^{-5}$ Torr. This enabled to widen the limits of considered \bar{n}_{e0} values from $3.5 \times 10^{12} \text{ cm}^{-3}$ at $t_0 = t_1 = 26$ ms (Fig. 5,a, regime 1) to $5.7 \times 10^{12} \text{ cm}^{-3}$ at $t_0 = t_1 = 30$ ms (see Fig. 5,b, regime 2) and to

$6.4 \times 10^{12} \text{ cm}^{-3}$ at $t_0 = 28 \text{ ms}$ and $t_1 = 30 \text{ ms}$ (see Fig. 5,c, the THTA pulse was applied to the afterglow plasma).

The initial ECE decayed with \bar{n}_{e0} increase. Basing on the Sec. 3 data, one can suppose, however, that in the conditions under consideration where $\max \bar{n}_e \sim (7 \dots 8) \times 10^{12} \text{ cm}^{-3}$ is achieved with THTA in operation (see Figs. 5,b,c) and T_e estimation by ECE becomes incorrect, the electron temperature also weakly depends on the initial value.

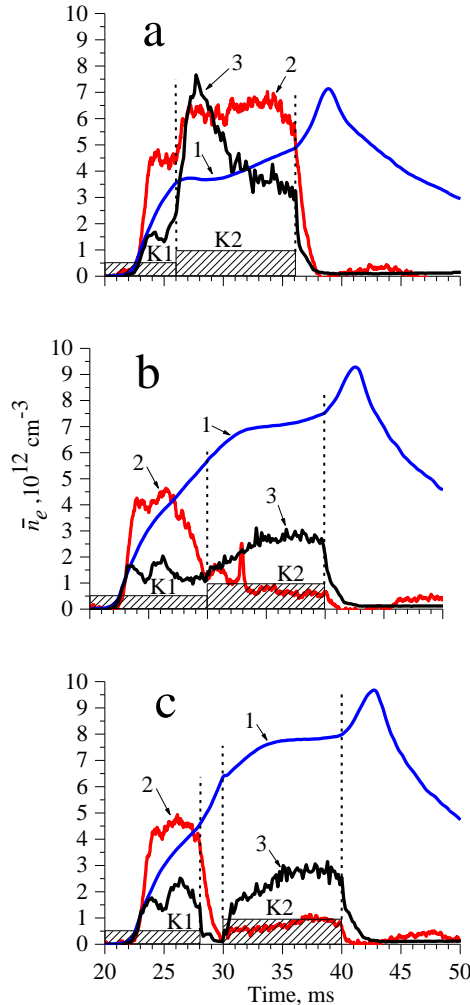


Fig. 5. Time evolution of 1, mean electron density \bar{n}_e , 2, 2nd harmonic ECE, 3, PDF current I_s depending on the times t_0 of K1 switched off and t_1 of K2 switched on: (a) $t_1 = t_0 = 26 \text{ ms}$; (b) $t_1 = t_0 = 30 \text{ ms}$; (c) $t_0 = 28 \text{ ms}$, $t_1 = 30 \text{ ms}$. The mean electron density is in units of 10^{12} cm^{-3} , while the other signals are in arbitrary units

At the lowest value $\bar{n}_{e0} = 3.5 \times 10^{12} \text{ cm}^{-3}$ (see Fig. 5,a) with RF voltage applied to THTA, ECE undergoes ≈ 1.5 -fold increase from the initial value to ≈ 6.5 a.u. and afterwards weakly changes to the end of the RF pulse by analogy with the regime 1 of the initial discharge. At the same time, PDF (current I_s), after passing over the maximum in the 1st half of the THTA RF pulse, undergoes ~ 2 times decrease. The decrease of the plasma loss results in a density rise to $\bar{n}_e = 5.0 \times 10^{12} \text{ cm}^{-3}$. As it has been already mentioned

above (see Sec. 2 and Fig. 2,d), this is an indication of plasma confinement improvement at a relatively high electron temperature. With a higher $\bar{n}_{e0} \sim 6 \times 10^{12} \text{ cm}^{-3}$, the density \bar{n}_e increases during the THTA pulse to $\sim 8.0 \times 10^{12} \text{ cm}^{-3}$ (see Figs. 5,b,c). Taking account of a relatively high PDF level in the active phase of the discharge and a finite, though lower, level of ECE together with a short-time \bar{n}_e rise after RF pulse termination, some electron heating could be supposed to occur in these conditions as well.

SUMMARY AND DISCUSSION

To find out possible regimes of the RF discharge driven by the three-half-turn antenna (THTA), time evolution has been studied of the average electron density \bar{n}_e , the intensity of the electron cyclotron emission ECE (radiation temperature) from the central region of the plasma column, and the plasma loss from the confinement volume (plasma divertor flow PDF – current I_s) depending on the frame-antenna-produced initial values of ECE and the mean density \bar{n}_{e0} as well as RF power P_{K2} fed to the antenna (anode voltage U_{K2} of the oscillator K2).

With fixed or weakly varying for the time of measurements initial plasma parameters and low values of P_{K2} (voltage U_{K2}), the THTA-driven discharge is in the regime similar to the regime 2 of the initial discharge (see Figs. 2,a,b). In this regime \bar{n}_e continues to grow and passes over the maximum $\approx (8 \dots 8.5) \times 10^{12} \text{ cm}^{-3}$. Judging on the low plasma loss, during the most part of the RF pulse the plasma remains cold, while the predominant fraction of the RF power P_{K2} coming to the confinement volume is spent for ionization of the neutral hydrogen, continuously entering this volume from the ambient space, as it has been already discussed in [6] for the FA-antenna-produced discharge.

With P_{K2} increasing, heating of the plasma (in part electrons, by the level of ECE) results in the loss increase, that is evidenced by slowing-down of the \bar{n}_e rise and the PDF increase. Finally, at a fixed pressure p the loss of the plasma is no more compensated by ionization of the coming neutrals. The slowing down of the density rise is replaced by its decay, and the mean plasma density lowers to $\bar{n}_e \sim 4 \times 10^{12} \text{ cm}^{-3}$ in the middle of the RF pulse, with T_e^{rad} being approximately 2 times as high as the initial one (see Figs. 2,c,d). As a result, the discharge goes to the regime similar to the regime 1 during FA operation [6]. A new effect here are indications of the hot plasma confinement improvement during evolution of the THTA-driven discharge.

With RF voltage being applied to THTA at different values of the initial ECE, it is shown that the resultant heating of the electrons weakly depends on their initial temperature (see Fig. 4). As follows from Figs. 4,c,d a high heating occurs even at ultimately low values of the initial electron temperature.

Basing on results of studies of the density \bar{n}_{e0} effect on the density and temperature of the THTA-driven

plasma with using available diagnostics, we can state reliably that a plasma with high radiation temperature and the density up to $\bar{n}_e \sim 5 \times 10^{12} \text{ cm}^{-3}$ can be produced within the range of $\bar{n}_{e0} \approx (3.5 \dots 5) \times 10^{12} \text{ cm}^{-3}$ (see Fig. 5,a, see, also, [8]) against $\bar{n}_e \sim (1 \dots 3) \times 10^{12} \text{ cm}^{-3}$ in the FA-produced discharge in the regime 1 [6]. At $\bar{n}_{e0} > 5 \times 10^{12} \text{ cm}^{-3}$ the mean density produced by THTA can be raised to $\sim 8 \times 10^{12} \text{ cm}^{-3}$. However, the method of electron temperature estimation used here does not allow to deduce a reliable conclusion about the level of electron heating at such a high density. Nevertheless, with the final values of ECE and plasma loss together with the mean electron density rise after the end of RF pulse (see Figs. 5,b, c) taken into account, a certain plasma heating with THTA should be expected even at $\bar{n}_e \sim 8 \times 10^{12} \text{ cm}^{-3}$. It seems that to realize the problem which THTA has been designed for, namely, production of the hot plasma with the mean density up to $\sim 10^{13} \text{ cm}^{-3}$, it is the regimes shown in Figs. 5,b, c that are the most promising.

When saying about optimum parameters of the initial frame-antenna-driven discharge to produce denser and hotter plasmas with the three-half-turn antenna, a conclusion could be made that even an afterglow plasma can be used as a target. This allows to produce the initial plasma using an ultimately low RF power P_{KI} that provides a stable discharge ignition and

brings the initial mean density to $\sim (5 \dots 6) \times 10^{12} \text{ cm}^{-3}$ in the regime 2.

REFERENCES

1. O.M. Shvets, I.A. Dikij, S.S. Kalinichenko, et al. // *Nucl. Fusion*. 1986, v. 26, p. 23.
2. V.V. Chechkin, L.I. Grigor'eva, M.S. Smirnova, et al. // *Nucl. Fusion*. 2002, v. 42, p. 192.
3. V.V. Chechkin, I.M. Pankratov, L.I. Grigor'eva, et al. // *PAST. Ser. "Plasma Physics"*. 2012, № 6, p. 3.
4. V.E. Moiseenko // *VIII IAEA Stellarator Workshop, Kharkov*, 1991, Vienna: IAEA, 1991, p. 207.
5. S.V. Kasilov, A.I. Lysoivan, V.E. Moiseenko, V.V. Plyusnin // *Stellarator and Other Helical Confinement Systems. Collection of Papers Presented at the IAEA TCM, Garching, Germany, 10-14 May 1993*. Vienna: IAEA, 1993, p. 277.
6. V.V. Chechkin, L.I. Grigor'eva, R.O. Pavlichenko, et al. // *Plasma Phys. Reports*. 2014, v. 40, № 8, p. 697.
7. A.I. Lysoivan, V.E. Moiseenko, V.V. Plyusnin, et al. // *Fusion Eng. Des.* 1995, v. 26, p. 185.
8. V.E. Moiseenko, V.L. Berezhnyj, V.N. Bondarenko, et al. // *Nucl. Fusion*. 2011, v. 51, p. 083036.
9. V.S. Voitsenya, A.N. Shapoval, R.O. Pavlichenko, et al. // *Phys. Scr.* 2011, v. T161, p. 014009.

Article received 20.09.2014

ХАРАКТЕРНЫЕ СВОЙСТВА ВЧ-РАЗРЯДА, ПОДДЕРЖИВАЕМОГО ТРЕХПОЛУВИТКОВОЙ АНТЕННОЙ В ТОРСАТРОНЕ УРАГАН-3М

В.В. Чечкин, Л.И. Григорьева, Д.Л. Греков, Р.О. Павличенко, А.В. Лозин, А.А. Касилов, А.А. Белецкий, М.М. Козуля, А.Е. Кулага, Н.В. Заманов, И.К. Тарасов, Ю.К. Миронов, В.С. Романов, В.С. Войцены

В трехзаходном торсатроне Ураган-3М водородная плазма создается и нагревается ВЧ-полями в области альфвеновских частот ($\omega \lesssim \omega_{ci}$). Плазма со средней плотностью \bar{n}_e единицы 10^{12} cm^{-3} создается рамочной антенной и используется как исходная для получения и нагрева более плотной плазмы (до $\bar{n}_e \sim 10^{13} \text{ cm}^{-3}$) с помощью более коротковолновой трехполувитковой антенны с азимутальными токами. Экспериментально исследуются характеристики ВЧ-разряда, поддерживаемого трехполувитковой антенной, в зависимости от ВЧ-мощности, подводимой к антенне, и параметров исходной плазмы.

ХАРАКТЕРНІ ВЛАСТИВОСТІ ВЧ-РОЗРЯДУ, ЩО ПІДТРИМУЄТЬСЯ ТРЬОХНАПІВВИТКОВОЮ АНТЕННОЮ В ТОРСАТРОНІ УРАГАН-3М

В.В. Чечкін, Л.І. Григор'єва, Д.Л. Греков, Р.О. Павличенко, О.В. Лозін, А.А. Касілов, О.О. Білецький, М.М. Козуля, А.Є. Кулага, М.В. Заманов, І.К. Тарасов, Ю.К. Миронов, В.С. Романов, В.С. Войцены

У трьохзаходному торсатроні Ураган-3М воднева плазма створюється і гріється ВЧ-полями в області альфвенівських частот ($\omega \lesssim \omega_{ci}$). Плазма з середньою щільністю \bar{n}_e одиниці 10^{12} cm^{-3} створюється рамковою антенною і використовується як початкова для одержання та нагріву щільнішої плазми (до $\bar{n}_e \sim 10^{13} \text{ cm}^{-3}$) за допомогою більш короткохвильової трьохнапіввиткової антени з азимутальними струмами. Експериментально досліджуються характеристики ВЧ-розряду, який підтримується трьохнапіввитковою антенною, в залежності від ВЧ-потужності, що підводиться до антени, та параметрів початкової плазми.